DOI: 10.1002/chem.200903526

Water Stable Zr–Benzenedicarboxylate Metal–Organic Frameworks as Photocatalysts for Hydrogen Generation

Cláudia Gomes Silva, Ignacio Luz, Francesc X. Llabrés i Xamena,* Avelino Corma, and Hermenegildo García*[a]

Abstract: The Zr-containing metal–organic frameworks (MOFs) formed by terephthalate (UiO-66) and 2-aminoterephthalate ligands [UiO-66(NH_2)] are two notably water-resistant MOFs that exhibit photocatalytic activity for hydrogen generation in methanol or water/methanol upon irradiation at wavelength longer than 300 nm. The apparent quantum yield for H_2 generation using monochromatic light at 370 nm in water/methanol 3:1 was of 3.5% for UiO-66(NH_2). Laser-flash photolysis has allowed detecting for UiO-66 and UiO-66(NH_2) the photochemical generation of a long lived charge separated state whose decay is not complete 300 μs after the laser flash. Our finding and particularly the influence of the amino group producing a bathochromic shift in the optical spectrum without altering the photochemistry shows promises for the development of more efficient MOFs for water splitting.

Keywords: hydrogen · metal–organic frameworks · photocatalysts · zirconium

Introduction

The synthesis and applications of metal–organic frameworks (MOFs) has emerged as a topic of much current interest due to the large flexibility in the preparation, the possibility to apply rational design, the large surface area and pore volume, the high metal content of the materials as well as some other properties.[1–8] MOFs are crystalline solids in where metal ions or metal clusters are linked to multi-topical organic linkers forming an extended three-dimensional structure.[2,4,9,10] Some of the structures described for MOFs are isoreticular with zeolites and crystalline aluminophosphates, but MOFs surpass the properties of zeolites in terms of porosity and low framework density. Recently, we have been exploring[11–13] the possibility of using MOFs as semiconductors in where photon absorption produces a state of charge separation with a positive hole in the valence band and an electron in the conduction band. This semiconducting behavior of MOFs is also unique among the microporous solids since zeolites and related materials are photochemically inert and behave as insulators.[14]

A general application of semiconductors is in photocatalysis in where the energy of light is converted into chemical energy.[15–17] Thus we have found that MOF-5 ($[Zn_4(O)(bdc)_3]$, BDC: 1,4-benzenedicarboxylate) exhibits a reverse shape selective activity in the photocatalytic degradation of phenols in where those phenols that can diffuse inside the micropore volume of MOF-5 are degraded slower compared to those that can not enter into the pores.[11,13] Similarly, Gascon et al.[18] have reported the use of isoreticular MOFs as tunable bandgap photocatalyst for the aerobic epoxidation of propylene. Also the photocatalytic activity of MOFs containing Cd^{2+}, Mn^{2+}, Gd^{3+} and Cu^{2+} for the degradation of dyes has recently been reported.[19,20] Following the exploitation of MOFs as photocatalysts, in the present manuscript we describe the activity for the photocatalytic hydrogen generation of two zirconium containing MOFs: UiO-66 ($[Zr_6O_4(OH)_4(bdc)_{12}]$)[21] and UiO-66($NH_2$) ($[Zr_6O_4(OH)_4(ata)_{12}]$, ATA: 2-aminoterephthalate). These two materials are isoreticular and they both feature a crystalline structure constituted by hexameric Zr_6O_{32} units. The six Zr atoms define a regular octahedron, in which the triangular faces alternatively contain μ_3-O and μ_3-OH capping groups. The octahedra are linked through 12 BDC (or ATA) ligand molecules, thus defining two types of cages: a supertetrahedron and a superoctahedron. Access to the internal surface of the material is possible through triangular windows of about

[a] Dr. C. Gomes Silva, I. Luz, Dr. F. X. Llabrés i Xamena, Prof. Dr. A. Corma, Prof. Dr. H. García
Instituto de Tecnología Química, CSIC-UPV
Universidad Politécnica de Valencia
Consejo Superior de Investigaciones Científicas
Av. de los Naranjos s/n, 46022 Valencia (Spain)
E-mail: hgarcia@qim.upv.es

Supporting information for this article is available on the WWW under http://dx.doi.org/10.1002/chem.200903526.

0.6 nm. Figure 1 shows a graphical representation of the crystal structure of UiO-66.

One of the most important properties of UiO-66 is their structural stability in water. It is known that MOF-5 undergoes transformation into other crystalline structures when exposed to moisture and water.[22] This structural change is reflected also in remarkable variations in their photophysical properties including emission spectra and time-resolved absorption spectra.[23] In contrast, UiO-66 has the advantage that can be suspended in water even at 100 °C for 4 h without producing any change in the structure of the MOF, as we have observed in our lab. This exceptional stability opens the possibility to use this and related zirconium MOFs as photocatalysts in water.

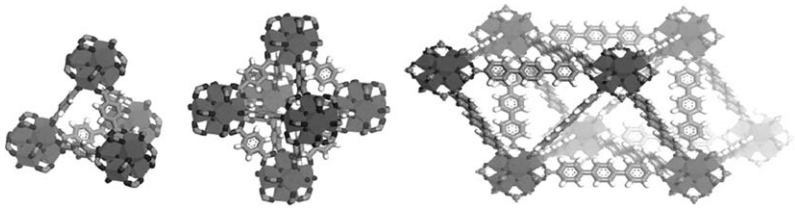

Figure 1. Crystal structure of UiO-66 (Reproduced with permission from ref. [21]).

In the present article, we describe the photocatalytic hydrogen generation of water/methanol using UiO-66 as photocatalyst. Moreover, we show that this photocatalytic activity can be increased by rational design of the material and by adding a hydrogen evolution co-catalyst. By using laser flash photolysis, the photocatalytic activity for hydrogen formation has been correlated with the generation of charge separated states.

Experimental Section

Synthesis and characterization of UiO-66 and UiO-66(NH_2): UiO-66 has been prepared following the procedure described by Cavka et al.[21] $ZrCl_4$ (53 mg, 0.227 mmol) and 1,4-benzenedicarboxylic acid (34 mg, 0.227 mmol) were dissolved in DMF (25 mL), and the solution was heated inside an autoclave at 120 °C for 48 h. After this time, the autoclave was cooled to room temperature in air (natural cooling). The recovered solid was washed with DMF and dried at room temperature under reduced pressure. Before using the Zr–MOF for the photocatalytic reactions, the occluded DMF molecules were eliminated by repeated washing with CH_2Cl_2, followed by drying under vacuum (100 °C, 12 h). The final yield obtained was 97% (dry basis). Elemental analysis was performed on the degassed $[Zr_6O_4(OH)_4(bdc)_{12}]$: calcd (%) for: C 43.52, H 1.96, N 0; found: C 43.89, H 2.13, N 0.62. The amount of zirconium in the final solid was determined by ICP-AES: calcd (%) for: Zr 20.68; found: Zr 20.01.

Preparation of the material UiO-66(NH_2) was achieved by replacing H_2BDC by H_2ATA, while keeping all other synthetic conditions unchanged. The final yield obtained was 94% (dry basis). Elemental analysis was performed on the sample washed with CH_2Cl_2 and outgassed under vacuum (100 °C, 12 h). $[Zr_6O_4(OH)_4(ata)_{12}]$: calcd (%) for: C 40.74, H 2.26, N 5.94; found: C 40.98, H 2.43, N 6.01. The amount of zirconium in the final solid was determined by ICP-AES: calcd (%) for: Zr 20.31; found: Zr 19.98.

The crystalline structure of the MOFs was checked by X-ray diffraction, using a Philips X'Pert MPD diffractometer equipped with a PW3050 goniometer ($Cu_{K\alpha}$ radiation, graphite monochromator) provided with a variable divergence slit.

Preparation of colloidal platinum nanoparticles: Colloidal platinum nanoparticles were produced based on a procedure described elsewhere[24] by adding dropwise an aqueous solution of H_2PtCl_6 (60 mg in 20 mL of water) to a methanol solution containing ascorbic acid (600 mg in 180 mL of methanol). The mixture was stirred at 90 °C for 3 h under reflux. After cooling, the suspension was centrifuged and the solid was washed twice with fresh methanol (5 mL). Then the solid was dried at room temperature and finally it was resuspended in water.

Photocatalytic reactions: The photocatalytic experiments were carried out in a 30 mL Pyrex reactor. The headspace of the reactor was connected to an inverted burette filled with water at atmospheric pressure, allowing the measurement of the evolved gas. In the photocatalytic reactions, Zr–MOFs powder (45 mg) was dispersed in water/methanol 3:1. The total volume of the suspensions was of 22.5 mL. The suspensions were purged with an argon flow for at least 30 min before irradiation in order to remove dissolved air. Then the suspensions were irradiated for 3 h using a 200 W xenon-doped mercury lamp (Hamamatsu Lightningcure LC8). The stationary temperature of the reactor was 38 °C. The formation of hydrogen was confirmed by injecting 0.5 mL of the reactor headspace gas in a gas chromatograph (HP 5890) operating at isothermal conditions (50 °C) using a semi-capillary column (molecular sieve, 530 μm diameter, 15 m length) equipped with a thermal conductivity detector. Photon flux was determined at 370 nm using a monochromator (half width 12 nm) by potassium ferrioxalate actinometry, and a value of 7.23×10^{-5} μmol photon s^{-1} was obtained.

Blank experiments, in the absence of any catalyst, were performed in order to evaluate the amount of hydrogen evolved directly from irradiation of the methanol/water mixtures. For comparison purposes, the volume of hydrogen generated from methanol/water photolysis was then deducted from the volumes generated in the presence of the catalysts. Therefore, the results presented here refer exclusively to the amounts of hydrogen generated from water/methanol mixtures by the photocatalytic route. Also we have included a control in which the photocatalytic activity of Zr–MOFs has been compared to that of P25 TiO_2 under the same conditions.

Results and Discussion

Visible light irradiation of UiO-66 suspensions in methanol/water do not allow the detection of any hydrogen evolution. Also using Pyrex filtered UV light as excitation source, UiO-66 as photocatalyst and water as hydrogen precursor in the absence of sacrificial electron donor do not form detectable H_2 amounts. In contrast, using Pyrex filtered UV light as radiation source in water/methanol mixtures, photocatalytic generation of H_2 was observed. Methanol should act as sacrificial electron donor being the source of the electrons required in the reduction semi-reaction of water. This contrasting behavior as a function of the excitation wavelength can be easily rationalized based on the optical spectrum of

UiO-66 that has a band at λ_{max} around 270 nm tailing beyond 300 nm.

In an attempt to increase the ability of UiO-66 to generate hydrogen, we synthesized an analogous MOF material using aminoterephthalate instead of terephthalate as linker [UiO-66(NH_2)]. We reasoned that the amino substituent acting as an auxochromic and bathochromic group in the aromatic ring should shift the absorption wavelength of the parent UiO-66. Figure 2 provides a comparison of the optical spectrum of UiO-66(NH_2) with that of UiO-66. As it was anticipated in our simple design, the spectrum of UiO-66-(NH_2) shows that the presence of the amino group originates an intense absorption band from 300 to 440 nm peaking at 360 nm, which is responsible for the yellow color of the solid. In view of the remarkable difference in the optical spectra of UiO-66 and UiO-66(NH_2), one could also assume that the presence of an amino group on the terephthalate linker promotes charge transfer interactions in the MOF.

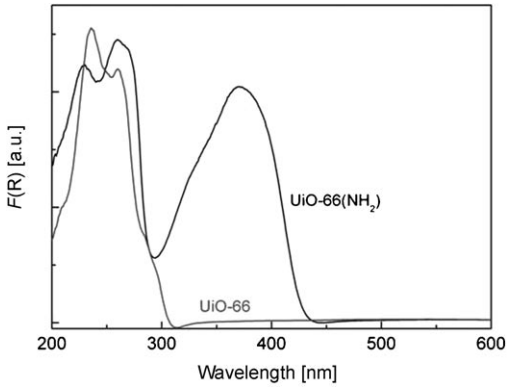

Figure 2. UV/Vis spectra of UiO-66 and UiO-66(NH_2) MOFs.

The materials UiO-66 and UiO-66(NH_2) are isoreticular, as confirmed by the total coincidence of the diffraction peaks of both solids, as shown in Figure 3. This coincidence of the XRD patterns indicates that the presence of the NH_2 does not play any influence on the structure of the MOF and that the NH_2 groups should be protruding into the empty space of the micropores. According to these data the main influence of the NH_2 is the appearance of a new desirable absorption band in the optical spectrum.

As it could be anticipated based on the increase in the light absorption by the presence of the NH_2 groups in the linker, photocatalytic tests show that UiO-66(NH_2) exhibits enhanced activity for hydrogen generation in water/methanol mixtures. Figure 4 provides a comparison of the temporal profile of hydrogen evolution using the same amounts of UiO-66 and UiO-66(NH_2) as photocatalyst.

In order to increase further the efficiency of the material as a photocatalyst for hydrogen evolution we anticipated that platinum nanoparticles acting as catalyst of hydrogen formation could enhance the efficiency of the system. As expected Figure 4 shows that for both MOFs UiO-66 and UiO-66(NH_2) the presence of Pt increases significantly the

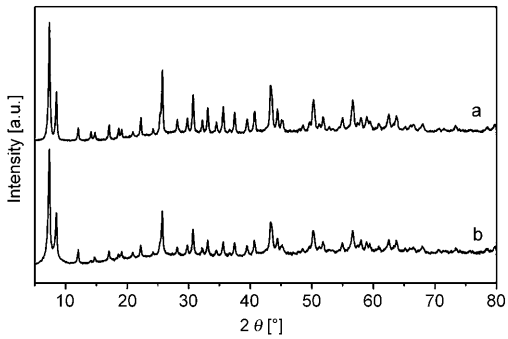

Figure 3. XRD patterns of UiO-66 (a) and UiO-66(NH_2) (b) MOFs.

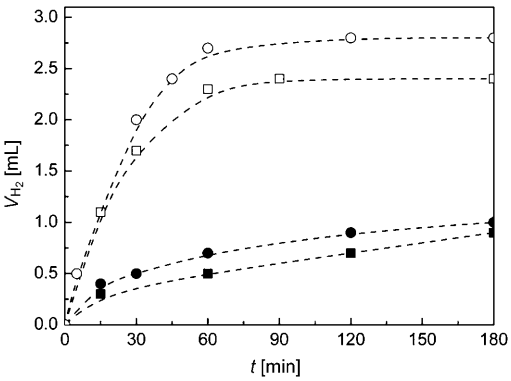

Figure 4. Volume of hydrogen evolved (V_{H2}) during he photocatalytic reactions using UiO-66 (■), UiO-66/Pt (□), UiO-66(NH_2) (●) and UiO-66-(NH_2)/Pt (○).

initial reaction rate and the total amount of hydrogen evolved in the irradiation. However, we notice that for both MOFs even though the initial rate of hydrogen formation increases the temporal evolution shows that the system becomes deactivated. Maximum amounts of 2.4 and 2.8 mL of H_2 have been obtained after 3 h of irradiation over UiO-66 and UiO-66(NH_2). For comparison, a maximum amount of 4.5 mL H_2 was obtained using TiO_2(P25) under identical experimental conditions (see Supporting Information).

As in a related precedent we attribute the deactivation of the photocatalytic system to the poisoning of by-products derived from methanol oxidation and particularly formic acid. To test this hypothesis a photocatalytic reaction under the same conditions but adding 1×10^{-2} M of formic acid leads to the inactivation of the photocatalytic activity of MOFs/Pt systems. This control confirms that as the hydrogen generation progresses, concomitant formation of oxidation products from methanol, and particularly formic acid, in increasing concentration deactivates the photocatalyst.

In an attempt to determine the hydrogen precursor and considering that pure water solutions do not form any H_2, we performed additional tests in which the percentage of methanol was increased from 0 to 100% vol. It was observed that pure methanol also forms H_2 under the photocatalytic conditions tested. However, the volume of evolved

hydrogen after 3 h irradiation in pure methanol as well as the initial reaction rate of H_2 evolution are lower than when using mixtures of water and methanol in the appropriate proportion. Figure 5 shows the time/conversion plot for H_2 evolution as a function of the composition of the liquid phase.

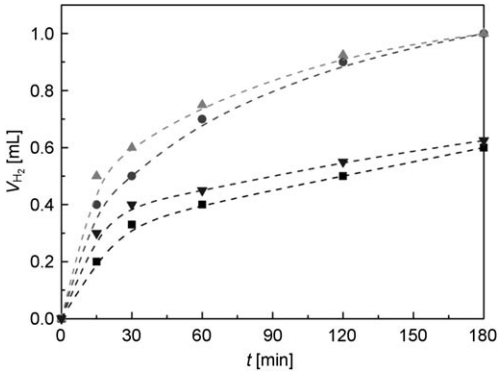

Figure 5. Volume of hydrogen evolved (V_{H_2}) using UiO-66(NH_2) as a function of the MeOH concentration (■: 10, ●: 33, ▲: 50, ▼: 100 vol%).

Similar results were observed when UiO-66 instead of UiO-66(NH_2) was used as the photocatalyst, indicating that this is a general effect. The above results clearly suggest that methanol is the most likely source of hydrogen, but that the presence of water enhances the photocatalytic activity.

Using monochromatic light of 370 nm, we determined the apparent quantum yield for H_2 evolution in a mixture of water and methanol (3:1) for UiO-66 and UiO-66(NH_2). This excitation wavelength was selected because it corresponds to the absorption maximum of UiO-66(NH_2). As it can be seen in Figure 2, at this wavelength the absorbance of UiO-66 is very low. Using ferrioxalate as chemical actinometer,[25] the quantum yield for H_2 evolution for UiO-66(NH_2) and UiO-66 were 3.5 and less than 0.1%, respectively. Although these values are far from optimum, they clearly show photocatalytic activity for UiO-66(NH_2) at this relatively long irradiation wavelength. Moreover, the difference in photocatalytic activity between UiO-66 and UiO-66(NH_2) nicely exemplifies the possibilities that modification of the linker offer to further improve the photocatalytic activity besides the design of other MOFs with different metal ions or clusters.

We propose that the photocatalytic activity of UiO-66 and UiO-66(NH_2) arises from their ability to act as semiconductors. There are some scattered examples in the literature in which some MOFs have exhibited semiconducting properties.[11,18–20,23,26–29] In previous works, the ability of MOFs and particularly MOF-5 to act as semiconductor has been already demonstrated.[11,23,30,31] Also precedents reporting the use of Co^{2+}, Mn^{2+} and Cu^{2+} MOFs as photocatalysts for dye degradation have proposed that UV photoexcitation leads to charge separation with electrons populating the LUMO (essentially corresponding to empty metal orbitals) and electron holes in the HOMO (considered in a simplified scheme as corresponding to the 2p orbitals of oxygen atoms).[19,20]

Laser flash photolysis using diffuse reflectance detection has been proved to be a powerful spectroscopic technique to detect photogenerated transients and particularly the states of charge separation characteristic of semiconductors.[27,29] In the present case we also performed a laser flash photolysis study of UiO-66 and UiO-66(NH_2) with the aim of having direct spectroscopic evidences of charge separation.

Using 355 nm laser excitation and performing the measurements under N_2, the formation of transients were detected. Figure 6 shows the time-resolved transient spectra recorded 9.5 μs after the laser flash. Both transient spectra for UiO-66 and UiO-66(NH_2) show some similarities with a continuous absorption from 300 to beyond 700 nm and relative maxima at 620 and 580 nm for UiO-66 and UiO-66(NH_2), respectively. The signals were very long-lived (see Figure 6) and their decay was not complete even after 300 μs, the longest lifetime available in our nanosecond laser system.

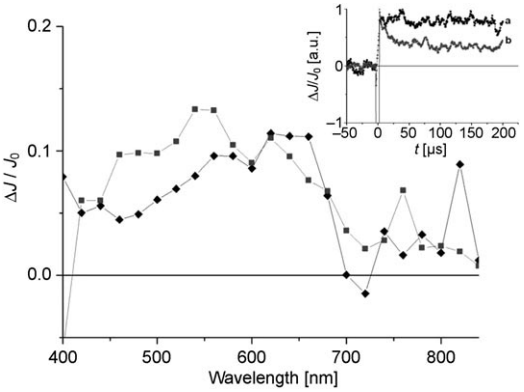

Figure 6. Time-resolved transient spectra recorded 9.5 μs after the laser flash corresponding to UiO-66 (◆) and UiO-66(NH_2) (■). Inset: Temporal profiles of the transient spectrum of UiO-66(NH_2) monitored at a) 480 and b) 560 nm.

Although for each MOF the temporal profiles of the signals exhibit some differences in the initial 30 μs depending on the wavelength being monitored, after this initial delay all the signal decays were parallel at all wavelengths monitored. This indicates that some fast transients could be present at short times after the laser pulse but once they have disappeared, there is a long-lived residual that must correspond to a single species or at two species decaying by mutual annihilation.

In order to provide some support on the nature of the transient species, particularly those long-lived that are better monitored in the available time-scale, we performed quenching experiments. As hole quenchers we used methanol and triethylamine, while as electron quenchers we used O_2 and N_2O. The transient spectra recorded in the presence

of quenchers changed, thus indicating that the assignment of the long-lived transient spectra to the charge separated species is reasonable. Figure 7 shows some transient spectra recorded in the presence of electron donor and acceptor quenchers. In particular we noticed that the effect of methanol and triethanolamine were coincident and lead to a continuous spectra without apparent relative maxima.

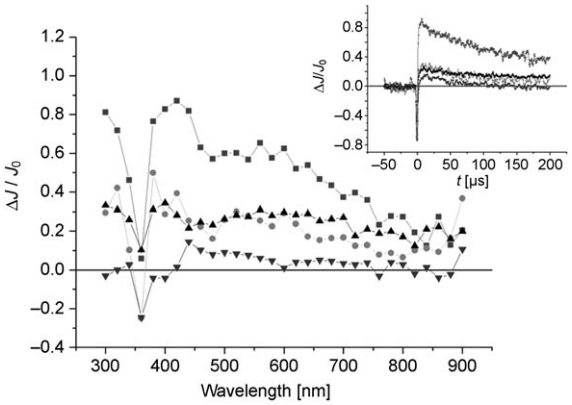

Figure 7. Transient spectra recorded for UiO-66(NH_2) in N_2 atmosphere and in the presence of different quenchers (■: N_2, ●: TEA, ▲: MeOH, ▼: O_2). Inset: Temporal profiles of the transient spectra monitored at 440 nm.

The signal intensity in the presence of the methanol and triethylamine quenchers was much lower due to the absence of positive holes, the residual signal being attributed to electrons delocalized in the conduction band of the semiconductor. In fact, there are precedents showing that electrons in the conduction band of semiconductors exhibit a continuous absorption over the whole wavelength range.[30–34] We also noticed that the residual was significantly much longer-lived. We interpret this fact considering that in the absence of quenchers, electron/hole recombination is the prevalent decay pathway. When the hole quencher is added, the decay of the electrons becomes slower because recombination is now considerably more difficult.

Interestingly, the effect of O_2 on the photogenerated transients is remarkable and almost leads to the complete signal disappearance. If O_2 were acting only as electron quencher, the transient spectra corresponding to holes should be observed. The fact that the transient spectra almost disappear suggests that besides as electron quencher O_2 is acting predominantly in another way. We propose that oxygen is inhibiting triplet excited states that would be at least in part the precursor of the charge separated state. In a related precedent concerning the photochemistry of MOF-5, it was determined by a combination of emission and laser flash photolysis that the triplet excited state was the precursor of charge separation.[11] We suggest that this is also applicable in our case. Scheme 1 summarizes the photophysics of the Zr–MOFs based on the available data.

Overall, the above spectroscopic evidence based on laser flash photolysis supports that Zr–MOFs can undergo long-lived charge separation that is the genuine prerequisite of semiconductors.

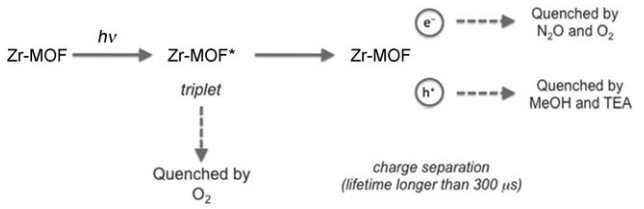

Scheme 1. Mechanistic proposal to rationalize the photophysics of the two Zr–MOFs under study. TEA = triethylamine.

Conclusion

MOFs are currently attracting much attention as materials for hydrogen storage, CO_2 sequestration and as solid catalysts. In the present work we have demonstrated the capability of water stable Zr–MOFs to act as photocatalysts for H_2 generation. Laser flash photolysis has detected long-lived transients that exhibit specific quenching characteristic of positive holes and electrons. We have interpreted the data to indicate that charge separation with electrons in the conduction band occurs upon photon absorption. The presence of the amino group in the BDC ligand does not influence the photochemistry but due to the auxochormic and bathochromic shift introduces an absorption in the wavelength longer than 300 nm. We have applied the remarkable water stability and semiconducting properties for photocatalytic hydrogen generation. Although the apparent quantum yield is still low, considering the large variety of structures and the combination of metals and linkers, our finding triggers a new research line aimed at exploiting MOFs as semiconductors, particularly for water splitting.

Acknowledgements

Financial support by the Spanish Ministry of Science and Innovation (CTQ 2009-11583) is gratefully acknowledged. C.G.S. thanks Fundação para a Ciência e a Tecnologia (Portugal) for a post-doctoral fellowship (SFRH/BPD/48777/2008). CSIC and Fundación Bancaja are acknowledged for a research contract to I.L.

[1] G. Férey, *Chem. Soc. Rev.* **2008**, *37*, 191–214.
[2] S. L. James, *Chem. Soc. Rev.* **2003**, *32*, 276–288.
[3] C. Janiak, *Dalton Trans.* **2003**, 2781–2804.
[4] S. Kitagawa, R. Kitaura, S. Noro, *Angew. Chem.* **2004**, *116*, 2388–2430; *Angew. Chem. Int. Ed.* **2004**, *43*, 2334–2375.
[5] J. Lee, O. K. Farha, J. Roberts, K. A. Scheidt, S. T. Nguyen, J. T. Hupp, *Chem. Soc. Rev.* **2009**, *38*, 1450–1459.
[6] C. Sanchez, B. Julian, P. Belleville, M. Popall, *J. Mater. Chem.* **2005**, *15*, 3559–3592.
[7] D. J. L. Tranchemontagne, Z. Ni, M. O'Keeffe, O. M. Yaghi, *Angew. Chem.* **2008**, *120*, 5214–5225; *Angew. Chem. Int. Ed.* **2008**, *47*, 5136–5147.

[8] O. M. Yaghi, H. L. Li, C. Davis, D. Richardson, T. L. Groy, *Acc. Chem. Res.* **1998**, *31*, 474–484.
[9] S. Natarajan, S. Mandal, *Angew. Chem.* **2008**, *120*, 4876–4907; *Angew. Chem. Int. Ed.* **2008**, *47*, 4798–4828.
[10] J. J. Perry IV, J. A. Perman, M. J. Zaworotko, *Chem. Soc. Rev.* **2009**, *38*, 1400–1417.
[11] M. Alvaro, E. Carbonell, B. Ferrer, F. X. Llabrés i Xamena, H. Garcia, *Chem. Eur. J.* **2007**, *13*, 5106–5112.
[12] C. Gomes Silva, A. Corma, H. García, *J. Mater. Chem.* **2010**, *20*, 3141–3156.
[13] F. X. Llabrés i Xamena, A. Corma, H. Garcia, *J. Phys. Chem. C* **2007**, *111*, 80–85.
[14] A. Corma, H. Garcia, *Chem. Commun.* **2004**, 1443–1459.
[15] M. A. Fox, M. T. Dulay, *Chem. Rev.* **1993**, *93*, 341–357.
[16] M. R. Hoffmann, S. T. Martin, W. Y. Choi, D. W. Bahnemann, *Chem. Rev.* **1995**, *95*, 69–96.
[17] A. Mills, S. LeHunte, *J. Photochem. Photobiol. A* **1997**, *108*, 1–35.
[18] J. Gascon, M. D. Hernandez-Alonso, A. R. Almeida, G. P. M. van Klink, F. Kapteijn, G. Mul, *ChemSusChem* **2008**, *1*, 981–983.
[19] D. E. Wang, K. J. Deng, K. L. Lv, C. G. Wang, L. L. Wen, D. F. Li, *CrystEngComm* **2009**, *11*, 1442–1450.
[20] L. L. Wen, F. Wang, J. Feng, K. L. Lv, C. G. Wang, D. F. Li, *Cryst. Growth Des.* **2009**, *9*, 3581–3589.
[21] J. H. Cavka, S. Jakobsen, U. Olsbye, N. Guillou, C. Lamberti, S. Bordiga, K. P. Lillerud, *J. Am. Chem. Soc.* **2008**, *130*, 13850–13851.
[22] S. Hausdorf, J. Wagler, R. Mossig, F. O. R. L. Mertens, *J. Phys. Chem. A* **2008**, *112*, 7567–7576.
[23] T. Tachikawa, J. R. Choi, M. Fujitsuka, T. Majima, *J. Phys. Chem. C* **2008**, *112*, 14090–14101.
[24] P. A. Brugger, P. Cuendet, M. Grätzel, *J. Am. Chem. Soc.* **1981**, *103*, 2923–2927.
[25] S. L. Murov, I. Carmichael, G. L. Hug in *Handbook of Photochemistry*, 2nd ed., Marcel Dekker, New York, **1993**.
[26] C. Bohne, M. Barra, R. Boch, E. B. Abuin, J. C. Scaiano, *J. Photochem. Photobiol. A* **1992**, *65*, 249–265.
[27] S. Bordiga, C. Lamberti, G. Ricchiardi, L. Regli, F. Bonino, A. Damin, K. P. Lillerud, M. Bjorgen, A. Zecchina, *Chem. Commun.* **2004**, 2300–2301.
[28] M. Fuentes-Cabrera, D. M. Nicholson, B. G. Sumpter, M. Widom, *J. Chem. Phys.* **2005**, *123*, 5.
[29] L. Maretti, E. Carbonell, M. Alvaro, J. C. Scaiano, H. Garcia, *J. Photochem. Photobiol. A* **2009**, *205*, 19–22.
[30] T. Asahi, A. Furube, H. Masuhara, *Chem. Phys. Lett.* **1997**, *275*, 234–238.
[31] D. P. Colombo, R. M. Bowman, *J. Phys. Chem.* **1995**, *99*, 11752–11756.
[32] D. P. Colombo, R. M. Bowman, *J. Phys. Chem.* **1996**, *100*, 18445–18449.
[33] G. P. Lepore, C. H. Langford, J. Vichova, A. Vlcek, *J. Photochem. Photobiol. A* **1993**, *75*, 67–75.
[34] S. Tojo, T. Tachikawa, M. Fujitsuka, T. Majima, *J. Phys. Chem. C* **2008**, *112*, 14948–14954.

Received: December 22, 2009
Revised: April 21, 2010
Published online: August 4, 2010

